Research Article GU J Sci 37(2): 688-699 (2024) DOI: 10.35378/gujs.1348483

Gazi University

Journal of Science

http://dergipark.gov.tr/gujs

Electromagnetic Scattering by Arbitrarily Located Electric and/or Magnetic Conducting Double-Strip

Kamil KARACUHA[1,*], Vasil TABATADZE[2]

[1] *Istanbul Technical University, Department of Electrical Engineering, 34467, İstanbul, Türkiye*
[2] *Istanbul Technical University, Informatics Institute, 34467, İstanbul, Türkiye*

Highlights

- New resonance and its novel characteristics are noticed.
- Validation with Dirichlet and Neumann boundary conditions are obtained.
- The finite wedge problem is investigated in detail.

Article Info

Received: 23 Aug 2023
Accepted: 10 Oct 2023

Keywords

Diffraction
Double-strip
Finite wedge
Scattering
Semi-analytical

Abstract

The study presents electromagnetic scattering by arbitrarily located double strips with perfect electric and/or magnetic conducting surfaces. The study generalizes not only the physical dimension, location, and orientation of the strips but also, the boundary conditions on each strip are generalized and variable. It can be Dirichlet or Neumann boundary conditions. Since the study considers numerous parameters as the variable, the comparison between the present study and the literature is investigated in detail. Geometries such as parallelly located double strips with fractional boundary conditions, impedance double strips, and wedge problems are considered to compare. Besides, the proposed methodology is compared by the method of moments, the method of auxiliary sources, and the orthogonal polynomials approach. The suggested research investigates the electromagnetic scattering by finite wedge and arbitrarily located two strips with different boundary conditions and widths for the first time since each strip can have different widths and boundary conditions (Dirichlet or Neumann). The results reveal that the angle between the strips, the rotation of the strips, width of the strip have noticeable effects on the scattered field and total radar cross-sections. Between the strips, resonances are observed and their characteristics have a substantial dependency on the boundary conditions.

1. INTRODUCTION

Electromagnetic scattering plays a critical role in numerous applications ranging from the military, biomedical, remote control, aviation, forecasting, and characterization. The scattering by finite objects or obstacles with edges is the preliminary and essential geometries for electromagnetic scattering [1]. Especially, in the twentieth century, vast and extensive analytical, numerical, and analytical-numerical methods are proposed to solve problems such as half-plane, wedge, strip, circular strip, ring, disc, and their combination or variants. The main aim is to obtain and then solve a differential equation or integral equation system after applying boundary conditions while taking into account the radiation and the edge conditions to achieve a unique solution [2].

Parallel with the investigations regarding the geometries, the different boundary conditions, and source types are investigated [3]. Still in the literature, one of the essential problems, diffraction by a half-plane problem is investigated by different approaches [4- 6]. In [4, 5], the approximate analytical methods are proposed to obtain the scattered field. In [6], the total field is obtained by the combination of the scattered field from soft and hard surfaces. Besides half-plane, the wedge problem has been studied for more than 70 years considering the different cases such as boundary condition, excitation, combination with other geometries, layered-media case, etc. [7- 9]. Apart from half-plane and wedge problems, there are

*Corresponding author, e-mail: karacuha17@itu.edu.tr

geometries such as strips, ring, circular strip, and apertures and their combinations or variants. These problems have been solved with several approaches and have more practical outcomes since they can be employed in engineering designs [10- 14]. In these problems, the main aim was to obtain the scattered field and observe the far-field radiation characteristics. They could lead to having an engineering design motivation. In [11], electromagnetic scattering by a conductive disc structure via a 1D modified integral equation employing Fourier expansion was used. Sub-domain bases for induced current were used to solve integral equations. Besides, orthogonal polynomials depending on the geometries can be used to express the current distribution as done in [13]. Beyond the bounds, the surface characteristics and the boundary conditions for similar obstacles or scatterers are also very important to research areas. The same geometries with different boundary conditions or periodic, non-periodic, rough, or smooth surfaces for similar geometries have been investigated and their comparison are obtained by the numerical methods or the validations are revealed for the limit case of the boundary condition or surface characteristic [15- 17].

To deeply understand and manipulate wave interaction, material characterization, sensing and antenna design, and solution of the scattering phenomena especially, new mathematical approaches for solving the canonical problems play an important effect on engineering development. In particular, semi-analytical and approximate methods give insight into dominant effects, and practical and fast solutions to design constraints and trade-offs. Apart from various boundary conditions on canonical diffraction problems, there are numerous studies investigating the scattering by canonical geometries for different scenarios such as multilayer cylinders with oblique incidence excitation, moving thin conducting strips and plates employing the physical optics and moving conducting spheres [18- 20].

Electromagnetic scattering by strip or strips has a very special importance among the other canonical problems since its limit case covers numerous similar problems such as a wedge, half-plane, aperture, etc. Therefore, for decades, the same geometry has been investigated and numerous approaches have been proposed including semi-analytical or numerical methods [21- 23]. Many interesting phenomena can be investigated such as the effect of the position, angle, length, boundary condition, and periodicity of the strip. The article aims to answer several questions in detail since in the literature, there is no similar study for electromagnetic scattering by two strips with the variable position, length, and boundary condition. The present study mainly investigates E-polarized electromagnetic scattering by arbitrarily locating different size strips where each strip can be perfect electric conducting (PEC) and/or perfect magnetic conducting (PMC) surface. While the Dirichlet boundary condition is satisfied in one strip, the Neumann boundary condition may be satisfied in the other one. The variability of all: the boundary conditions, the angle between the strips, the lengths of the strips, and the center points puts the study in a place that covers and generalizes studies in the literature. The comparisons between the proposed methods with other studies in the sense of both methodology and geometry are presented. Advantage of the proposed approach to other studies is more strict mathematical solution because we require edge condition and also current is expanded in terms of orthogonal polynomials which makes it faster converging regarding the purely numerical methods. As a result our approach requires less computational memory complexity.

The study follows the formulation of the problem in which the mathematical manipulations and the details of the proposed method are covered. Then, the numerical outcomes and the comparisons with other methods are provided in the following chapter. Later, the conclusion is drawn.

2. FORMULATION OF THE PROBLEM

Formulation of the problem in which the mathematical expression for the field components due to each scatterer and the incident wave is formalized and after having the boundary condition (BC) satisfaction, the coupled integral equations are obtained. The proposed method would employ an orthogonal polynomials approach expressing the current distribution of the scatterer in terms of Gegenbauer polynomials. Then by Fourier transform and the orthogonality properties, the coupled integral equation system is transferred to a system of linear algebraic equations. By inversion, unknown coefficients are obtained and the current distribution is found. Then, the other physical properties such as radiation pattern, radar cross sections, and near-field distributions are obtained.

2.1. Mathematical Expressions and Geometry of the Problem

The problem consists of two strips located arbitrarily in the space with infinite length in the z-direction and infinitesimal thickness as given in Figure 1. The widths of the strips are $2a_i$. Here $i = 1, 2$. The incidence wave is an E-polarized plane wave. Due to having a two-dimensional problem, on the x-y plane, the center points of each strip are $\rho = l_i$ and $\phi = \theta_i$, respectively. Note that, the center points of each strip are given cylindrical coordinates variables (ρ, ϕ). Strips have their local coordinate systems as $(x_i,\ y_i)$ and they are rotated ϕ_i angle concerning the x-direction in the global coordinate system.

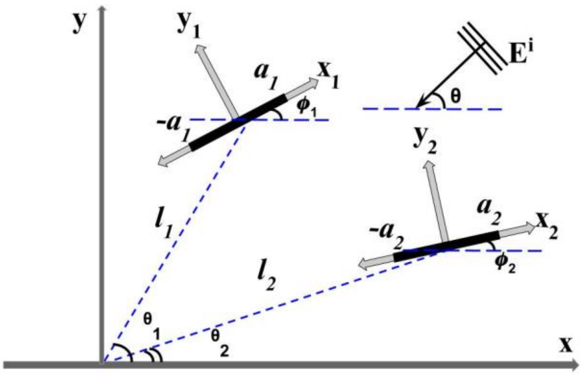

Figure 1. *The geometry of the problem*

$E_z(x, y)$ is the total electric field subjecting to Dirichlet or Neumann boundary conditions depending on the properties of strips as given in Equation (1). Strips can individually be PEC or PMC. For E-polarized electromagnetic scattering, the Dirichlet boundary condition stands for PEC surfaces whereas the Neumann boundary condition corresponds to the PMC surface

$$\vec{E}_z = \vec{E}_z^i + \vec{E}_z^s \tag{1}$$

where $\vec{E}_i = \vec{a}_z e^{-ik(x\cos\,\theta + y\sin\,\theta)}$. Here, $\vec{a}_z$ is the unit vector along the z-axis, θ is the angle of incidence, $k = 2\pi/\lambda$ is the wave number, and λ is the wavelength in free space. Note that the time dependency throughout this study is taken as $e^{-i\omega t}$ and then is omitted. The total electric field is the vector summation of the incidence wave $\vec{E}_z^i$ and the scattered electric field $\vec{E}_z^s$, respectively. The boundary conditions are required to find the total field in space. In other words, the tangential component of the electric field (in this problem, due to having an E-polarized incidence wave, the total electric field is already tangential for each local coordinate system) satisfies the Dirichlet or Neumann boundary conditions as given in Equation (2), respectively [24]:

$$E_z(x, y)|_{y_i=\pm 0} = 0,$$
$$\frac{\partial}{\partial k y_i} E_z(x, y)\Big|_{y_i=\pm 0} = 0 \tag{2}$$

where $x_i, -a_i < x_i < a_i$, $i = 1{,}2$. Here, $\vec{y}_i$ is the normal direction of the strips in their local coordinate systems. To have one compact definition, we can introduce a derivative operator D and a parameter ν_i that can both represent Dirichlet and Neumann boundary conditions as:

$$D_{ky_i}^{\nu_i} E_z(x, y)\Big|_{y_i=\pm 0} = 0. \tag{3}$$

Here $D_{ky_i}^{\nu_i}$ stands for the derivative operator $\frac{\partial}{\partial k y_i}$ and ν_i is the order of the derivative operator and could take a value of 0 or 1 depending on the boundary conditions. In other words, $\nu_i = 0$ cases, the Dirichlet boundary condition is satisfied whereas, $\nu_i = 1$ case, the Neumann boundary condition is represented mathematically. After this point, this operator would be employed for further derivations. This approach allows us to investigate the following cases: two PEC strips, two PMC strips, one PEC strip, and another PMC strip case.

To find the scattered electric field components due to each strip, the field components are expressed as the convolution of the unknown electric or magnetic current density f_i induced on each strip with the corresponding Green's function (G) [24]. Note that, currents only exist on the strips and we aim to find the unknown electric or magnetic current densities on the strip depending on the boundary conditions. Then, field components and later total field can be obtained easily by Equations (1) and (4).

$$E_z^{s,i}(x_i,y_i) = \int_{-\infty}^{\infty} f_i(x_i')D_{ky_i}^{\nu_i}G(x_i-x_i',y_i)dx_i', i = 1,2, \tag{4}$$

where $D_{ky_i}^{\nu_i}G^{\nu_i}(x_i-x_i',y_i) = \begin{cases} -\frac{i}{4}H_0^{(1)}\left(k\sqrt{\left(x_i-x_i'\right)^2+y_i^2}\right), & \nu_i = 0 \text{ (PEC case)} \\ -\frac{i}{4}\frac{\partial}{\partial ky_i}\, H_0^{(1)}\left(k\sqrt{\left(x_i-x_i'\right)^2+y_i^2}\right), & \nu_i = 1 \text{ (PMC case).} \end{cases}$

Here, $H_0^{(1)}$ is the Hankel function of the first kind and zero order. Since $D_{ky_i}^{\nu_i}$ is the derivative operator and the derivative of the exponents is easy to obtain, all field components (incident and scattered ones) are expressed in terms of the exponents and then, the spectral representation of the Hankel function is used as given in Equation (5):

$$H_0^{(1)}\left(k\sqrt{\left(x_i-x_i'\right)^2+y_i^2}\right) = \frac{1}{\pi}\int_{-\infty}^{\infty} e^{ik[(x_i-x_i')\alpha+|y_i|\sqrt{1-\alpha^2}]}\frac{d\alpha}{\sqrt{1-\alpha^2}} \quad . \tag{5}$$

After using the spectral representation of the Hankel function, the scattered field components can be expressed as below:

$$E_z^{i,s}(x_i,y_i) = -\frac{i}{4\pi}e^{\pm\frac{\pi\nu_i}{2}}\int_{-\infty}^{\infty} F_i(q)e^{ik\left[qx_i+|y_i|\sqrt{1-q^2}\right]}(1-q^2)^{\frac{\nu_i-1}{2}}dq, i = 1,2, \tag{6}$$

where:

$$F_i(q) = \int_{-1}^{1} \tilde{f}_i(\xi)e^{-i\epsilon_i q\xi}d\xi, \tilde{f}_i(\xi) = a_i f_i(a_i\xi),$$

$$\epsilon_i = ka_i, \xi = \frac{x_i}{a_i}, f_i(\xi) = \frac{\epsilon_i}{2\pi}\int_{-\infty}^{\infty} F_i(q)e^{-i\epsilon_i q\xi}dq,$$

$$\begin{bmatrix} x_i \\ y_i \end{bmatrix} = \begin{bmatrix} \cos\,\phi_i & \sin\,\phi_i \\ -\sin\,\phi_i & \cos\,\phi_i \end{bmatrix}\begin{bmatrix} x-l_i\cos\,\theta_i \\ y-l_i\sin\,\theta_i \end{bmatrix}.$$

By normalization, each strip ranges from -1 to 1 in their local coordinate system. Note that, Equation (6) satisfies both the wave equation and the Sommerfeld radiation condition where the (+) sign corresponds to the upper half space ($y_i > 0$) and (-) stands for the lower half-space ($y_i < 0$) for each local coordinate) [16]. The relation between local and global coordinate systems is also given in Equation (6).

In Equation (7), the incidence electric field and the scattered fields due to each strip are subject to the boundary condition on the corresponding strip as shown in Figure 1. Note that, to apply the boundary condition, all fields are expressed in the local coordinate system (x_i, y_i). Interaction terms are also transferred from a local coordinate system to another one $i, j = 1, 2,$ and $i \neq j$)

$$D_{ky_i}^{\nu_i}E_z^i\Big|_{y_i=0} = e^{-ik[\cos(\theta-\phi_i)x_i+l_i\cos(\theta-\theta_1)]}\left(-i\sin(\theta-\phi_i)\right)^{\nu_i},$$

$$D_{ky_i}^{\nu_i}E_z^{i,s}(x_i,y_i)\Big|_{y_i=0} = -\frac{i}{4\pi}e^{\pm i\frac{\pi\nu_i}{2}(i)^{\nu_i}}\int_{-\infty}^{\infty} F_i(q)e^{ik[qx_i]}(1-q^2)^{\nu_i-\frac{1}{2}}dq, \tag{7}$$

$$D_{ky_i}^{\nu_i} E_z^{j,s}(x_i, y_i)\Big|_{y_i=0} = -\frac{i}{4\pi} e^{\pm i\frac{\pi\nu_j}{2}} \int_{-\infty}^{\infty} F_j(q) e^{ik\left[q(Ax_i+\eta)+|Bx_i+\xi|\sqrt{1-q^2}\right]} \left[i(-B + A)\sqrt{1-q^2}\right]^{\nu_i} (1-q^2)^{\frac{\nu_j-1}{2}} dq,$$

where $A = \cos(\phi_j - \phi_i), B = \sin(\phi_j - \phi_i), \eta = l_i \cos(\theta_i - \phi_j) - l_j \cos(\theta_j - \phi_j), \xi = l_i \sin(\theta_i - \phi_j) - l_j \sin(\theta_j - \phi_j)$.

After applying the boundary conditions as given in Equation (3) and then, multiplying both sides of Equation (7) by $e^{-ikx_i\tau}$, an integral from $-a_i$ to $+a_i$ with respect to x_i is taken. Then, the integral equation (IE) for each strip becomes as ($i, j = 1, 2$ and $i \neq j$):

$$e^{-\frac{i\pi\nu_i}{2}} e^{-ikl_i\cos(\theta-\theta_i)} (\sin(\theta-\phi_i))^{\nu_i} \frac{\sin(\epsilon_i[\cos(\theta-\phi_i)+\tau])}{\cos(\theta-\varphi_1)+\tau} =$$

$$= \frac{i}{4\pi} e^{+\frac{i\pi\nu_i}{2}} \Bigg(e^{\pm i\frac{\pi\nu_i}{2}} \int_{-\infty}^{\infty} F_i(q) \frac{\sin(\epsilon_i[q-\tau])}{[q-\tau]} (1-q^2)^{\nu_i - \frac{1}{2}} dq$$
$$+ e^{\pm i\frac{i\pi\nu_j}{2}} \int_{-\infty}^{\infty} F_j(q) e^{ik\left[q\eta+\xi\sqrt{1-q^2}\right]} \frac{\sin\left(\epsilon_i\left[Aq+B\sqrt{1-q^2}-\tau\right]\right)}{\left[Aq+B\sqrt{1-q^2}-\tau\right]} \left[-Bq + A\sqrt{1-q^2}\right]^{\nu_i} (1-q^2)^{\frac{\nu_j-1}{2}} dq \Bigg). \quad (8)$$

After obtaining the IE for each strip, the Equation (8) needs to be solved for each strip. To solve this, there are some constraints taken into account such as edge and radiation conditions for the electromagnetic field. Note that, the scattered field given as Equation (6) already satisfies the radiation condition. The edge condition should be considered. Therefore, the electric or magnetic current density should be defined regarding the edge conditions. In other words, the current density at the edge of the strip should behave according to Meixner's edge condition. To satisfy Meixner's edge condition [25], the normalized fractional current density $\tilde{f}_i$ for each strip is expressed as the summation of Gegenbauer polynomials $C_n^{\nu_i}(\xi)$ with the weighting function $(1-\xi)^{\nu_i-1/2}$and the unknown coefficients $\zeta_n^{\nu_i}$ as in Equation (9). The reason why Gegenbauer polynomials are employed is that they are defined between [-1,1] and the weighting function is also suitable while finding unknown coefficients $\zeta_n^{\nu_i}$ by employing orthogonality properties of the corresponding polynomials [13, 24]

$$\tilde{f}_i(\xi) = (1-\xi)^{\nu_i - \frac{1}{2}} \sum_{n=0}^{\infty} \zeta_n^{\nu_i} \frac{C_n^{\nu_i}(\xi)}{\nu_i}, \quad (9)$$

where limits for ν_i is provided as [24- 26]

$$\lim_{\nu_i \to 0} \frac{C_n^{\nu_i}(\xi)}{\nu_i} = \begin{cases} \frac{2}{n} T_n(\xi), n \neq 0 \\ 1, n = 0 \end{cases}, \lim_{\nu_i \to 1} \frac{C_n^{\nu_i}(\xi)}{\nu_i} = C_n^1(\xi) = U_n(\xi).$$

Notice that T_n and U_n are the Chebyshev polynomials of the first and second kinds, respectively. Then, the Fourier transform of Equation (9) is obtained as [27]:

$$F_i(q) = \frac{2\pi}{\Gamma(\nu_i+1)} \sum_{n=1}^{\infty} (-i)^n \zeta_n^{\nu_i} \beta_n^{\nu_i} \frac{J_{n+\nu_i}(\epsilon_i q)}{(2\epsilon_i q)^{\nu_i}}. \quad (10)$$

Here, $\epsilon_i = ka_i$, $J_{n+\nu_i}(\epsilon_i q)$ are Bessel functions and $\beta_n^{\nu_i} = \Gamma(n+2\nu_i)/\Gamma(n+1)$ and $\Gamma(x)$ is the Gamma function. By substituting Equation (10) into Equation (8), multiplying by $\frac{J_{K+\nu_i}(\epsilon_i\tau)}{\tau^{\nu_i}}$and taking the integral with respect to τ from $-\infty$ to ∞ for each corresponding IE, the coupled integral Equation (8) is converted into the system of linear algebraic equation (SLAE) by introducing previously the unknown coefficients $\zeta_n^{\nu_i}$. Note that, here, the properties of discontinuous integrals of Weber-Shafheitlin Equation (11) are considered [26, 27]

$$\frac{1}{\pi}\int_{-\infty}^{\infty}\frac{J_{n+\alpha}(\epsilon q)}{q^{\alpha}}\frac{\sin\left(\epsilon(q\mp\beta)\right)}{(q\mp\beta)}dq=(\pm 1)^{n}\frac{J_{n+\alpha}(\epsilon\beta)}{\beta^{\alpha}}. \quad (11)$$

Then, coupled SLAE is obtained for each strip as:

$$\sum_{n=0}^{\infty}(-i)^{n}\zeta_{n}^{\nu_1}\beta_{n}^{\nu_1}C_{Kn}^{\nu_1\nu_1}+\mathcal{M}\sum_{n=0}^{\infty}\frac{(-i)^{n}\zeta_{n}^{\nu_2}\beta_{n}^{\nu_2}}{(2\epsilon_2)^{\nu_2}}C_{Kn}^{\nu_2\nu_1}=-\mathcal{R}(-1)^{K}e^{-ikl_1\cos(\theta-\theta_1)}(\sin(\theta-\varphi_1))^{\nu_1}\frac{J_{K+\nu_1}(\epsilon_1[\cos(\theta-\varphi_1)])}{[\cos(\theta-\varphi_1)]^{\nu_1}}, \quad (12)$$

$$\sum_{n=0}^{\infty}(-i)^{n}\zeta_{n}^{\nu_2}\beta_{n}^{\nu_2}C_{Kn}^{\nu_2\nu_2}+\mathcal{D}\sum_{n=0}^{\infty}\frac{(-i)^{n}\zeta_{n}^{\nu_1}\beta_{n}^{\nu_1}}{(2\epsilon_1)^{\nu_1}}C_{Kn}^{\nu_1\nu_2}=-\mathcal{P}(-1)^{K}e^{-ikl_2\cos(\theta-\theta_2)}(\sin(\theta-\varphi_2))^{\nu_2}\frac{J_{K+\nu_2}(\epsilon_2[\cos(\theta-\varphi_2)])}{[\cos(\theta-\varphi_2)]^{\nu_2}}, \quad (13$$

where $(i,j=1{,}2 \text{ and } i\neq j)$,
$\mathcal{M}=(2\epsilon_1)^{\nu_1}e^{\mp i\frac{\pi\nu_1}{2}}e^{\pm i\frac{\pi\nu_2}{2}}\frac{\Gamma(\nu_1+1)}{\Gamma(\nu_2+1)},\mathcal{R}=(2\epsilon_1)^{\nu_1}2ie^{-i\pi\nu_1}e^{\mp i\frac{\pi\nu_1}{2}}\Gamma(\nu_1+1),$
$\mathcal{D}=(2\epsilon_2)^{\nu_2}e^{\pm i\frac{\pi\nu_1}{2}}e^{\mp i\frac{\pi\nu_2}{2}}\frac{\Gamma(\nu_2+1)}{\Gamma(\nu_1+1)},\mathcal{P}=(2\epsilon_2)^{\nu_2}2ie^{-i\pi\nu_2}e^{\mp i\frac{\pi\nu_2}{2}}\Gamma(\nu_2+1),$
$C_{Kn}^{\nu_i\nu_i}=\left[\int_{-\infty}^{\infty}\frac{J_{n+\nu_i}(\epsilon_i q)}{q^{2\nu_i}}J_{K+\nu_i}(\epsilon_i q)(1-q^2)^{\nu_i-\frac{1}{2}}dq\right],$
$C_{Kn}^{\nu_i\nu_j}=\left[\int_{-\infty}^{\infty}\frac{J_{n+\nu_i}(\epsilon_i q)}{q^{\nu_i}}\frac{J_{K+\nu_j}\left(\epsilon_j\left(Aq+B\sqrt{1-q^2}\right)\right)}{\left(Aq+B\sqrt{1-q^2}\right)^{\nu_j}}e^{ik\left[q\eta+\xi\sqrt{1-q^2}\right]}\left[Bq-A\sqrt{1-q^2}\right]^{\nu_j}(1-q^2)^{\frac{\nu_i-1}{2}}dq\right].$

To solve SLAE, the summations are truncated for any desired accuracy. For the truncation in Equation (12) and Equation (13), $ka+6$ is chosen where a is the half-width of the wider strip [28]. After the unknown coefficients $\zeta_n^{\nu_i}$ are found by solving SLAE, corresponding scattered electric field can be found by using Equation (6) and Equation (10) in the local coordinate systems of each strip. Then, by coordinate transform, the scattered electric field $\vec{E}_z^s$ in the global coordinate system is obtained as Equation (14)

$$E_z^{1,s}(x,y)=H\int_{-\infty}^{\infty}F_1(q)e^{ik\left[q(x\cos\phi_1+y\sin\phi_1-l_1\cos(\theta_1-\phi_1))+|-x\sin\phi_1+y\cos\phi_1-l_1(\sin(\theta_1-\phi_1))|\sqrt{1-q^2}\right]}(1-q^2)^{\frac{\nu_1-1}{2}}dq$$
$$E_z^{2,s}(x,y)=H\int_{-\infty}^{\infty}F_2(q)e^{ik\left[q(x\cos\phi_2+y\sin\phi_2-l_2\cos(\theta_2-\phi_2))+|-x\sin\phi_2+y\cos\phi_2-l_2(\sin(\theta_2-\phi_2))|\sqrt{1-q^2}\right]}(1-q^2)^{\frac{\nu_2-1}{2}}dq \quad (14)$$

where $H=-\frac{i}{4\pi}e^{\pm i\frac{\pi\nu_1}{2}}$ and $T=-\frac{i}{4\pi}e^{\pm i\frac{\pi\nu_2}{2}}$.

2.2. Physical Characteristics of the Electric Field

In this section, the far-field radiation pattern (RP) of the total scattered field and the total radar cross-section (TRCS) expression are given. After finding the Fourier transform of the fractional current densities induced on each strip F_i, RP can be found by using the stationary phase method [29]. Note that it is valid for large values of ka ($ka\to\infty$). In Equation (15), $x=rcos\phi$ and $y=rsin\phi$

$$E_z^s(x,y)=A(kr)\Phi^{\nu}(\phi) \quad (15)$$

where $A(kr) = \sqrt{\frac{2}{\pi kr}} e^{ikr - i\frac{\pi}{4}}$ and $\Phi^{\nu} = -\frac{i}{4}(\pm)^{\nu} F(\cos\,\phi)\sin^{\nu}(\phi)$. In Equation (15), $\Phi^{\nu}(\phi)$ is denoted as the radiation pattern (RP). The upper sign in the $\Phi^{\nu}(\phi)$ expression corresponds to the upper space of each strip. On the other hand, the lower sign stands for the lower space where ϕ is the observation angle. $A(kr)$ stands for the radial and $\Phi^{\nu}(\phi)$ is the angular part of the total scattered electric field in the far zone. The angular part has two components because there are two scatterers in the space. Therefore, the total radiation pattern consists of two corresponding radiation patterns of each strip as Equation (16):

$$\Phi(\phi) = \Phi_1^{\nu_1}(\phi) + \Phi_2^{\nu_2}(\phi) \tag{16}$$

where

$$\Phi_1^{\nu_1}(\phi) = -\frac{\mathrm{i}}{4} e^{\pm\frac{i\pi\nu_1}{2}} [F_1(\cos\,\phi)](\sin^{\nu_1}(\phi - \phi_1))AF_1$$
$$\Phi_2^{\nu_2}(\phi) = -\frac{\mathrm{i}}{4} e^{\pm\frac{i\pi\nu_2}{2}} [F_2(\cos\phi)](\sin^{\nu_2}(\phi - \phi_2))AF_2\,. \tag{17}$$

Here, $AF_1 = e^{-ikl_1\cos(\theta_1 - \phi)}$ and $AF_2 = e^{-ikl_2\cos(\theta_2 - \phi)}$. Note that in Equation (17), the (+) sign for $\phi \in [\phi_i, \pi + \phi_i]$ and (-) for $\phi \in [\pi + \phi_i, 2\pi - \phi_i]$ as mentioned above [24]. After obtaining the total scattered electric field, the total radar cross-section can be evaluated to find the resonances and modes for different geometries. To find TRCS, Equation (18) is taken into account [30]:

$$\sigma_t = \frac{1}{ka}\int_0^{2\pi} |\Phi|^2 d\phi. \tag{18}$$

3. NUMERICAL RESULTS AND COMPARISONS WITH OTHER APPROACHES

In this part, the numerical results are presented and the comparison with other approaches is provided for the single or double parallel strips and wedge problems. To obtain a wedge, two strips are located closely regarding the wavelength. To observe resonance for different surfaces, TRCS is investigated in Figure 2. As expected, for the PMC surface, the resonances are more noticeable. In Figure 3, the normalized electric field values are provided for PEC-PMC and PMC-PMC cases at the resonance ka values. As is seen from the figures, the boundary conditions are satisfied. For Figure 3(a), the upper (lower) strip is PEC (PMC) where a tangential component of the total electric field vanishes for PEC surfaces whereas its normal derivative becomes zero for the PMC case. Figure 3 is provided after determining the resonances obtained from Figure 2. For Figure 3(a), the first resonance is given. However, the second resonance is provided for the PMC-PMC case.

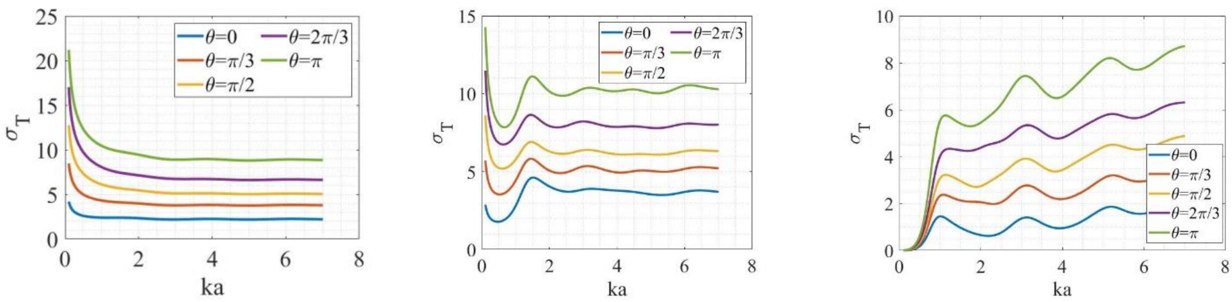

(a) $(\nu_{1,2} = 0.01, a_{1,2} = 1, \theta_{1,2} = \pm\frac{\pi}{4}, \phi_{1,2} = \pm\frac{\pi}{4}, l_{1,2} = 1.001)$

(b) $(\nu_1 = 0.01, \nu_2 = 1, a_{1,2} = 1, \theta_{1,2} = \pm\frac{\pi}{4}, \phi_{1,2} = \pm\frac{\pi}{4}, l_{1,2} = 1.001)$

(c) $(\nu_1 = 1, \nu_2 = 1, a_{1,2} = 1, \theta_{1,2} = \pm\frac{\pi}{4}, \phi_{1,2} = \pm\frac{\pi}{4}, l_{1,2} = 1.001)$

Figure 2. *TRCS for Finite Wedge: different cases (a) PEC-PEC (b) PEC-PMC (c) PMC-PMC*

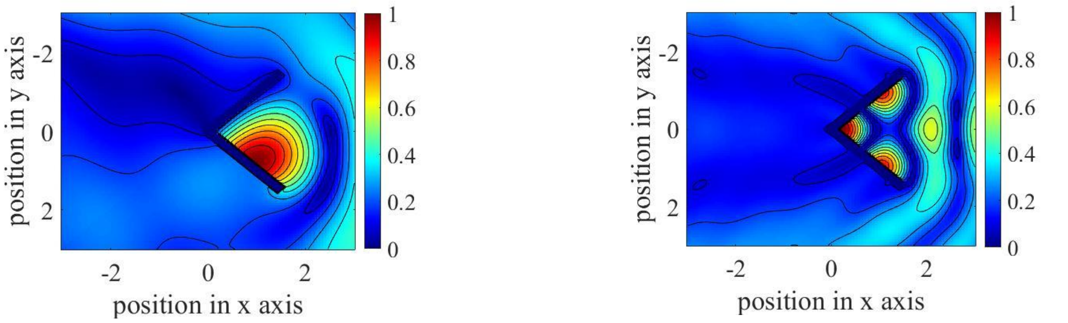

$(k = 1.49, \theta_0 = 0, \nu_1 = 0.01, \nu_2 = 1,$
$a_{1,2} = 1, \theta_{1,2} = \pm\frac{\pi}{4}, \phi_{1,2} = \pm\frac{\pi}{4}, l_{1,2} = 1.001)$
(a)

$(k = 3.14, \theta_0 = 0, \nu_1 = 1, \nu_2 = 1,$
$a_{1,2} = 1, \theta_{1,2} = \pm\frac{\pi}{4}, \phi_{1,2} = \pm\frac{\pi}{4}, l_{1,2} = 1.001)$
(b)

Figure 3. *Normalized near electric field distribution for Finite Wedge: different cases (a) PEC-PMC and (b) PMC-PMC*

In Figure 4, the comparison of the infinite and the finite wedge is illustrated. As expected, there exists deviation especially inside of the wedge since the electromagnetic waves can be diffracted from open ends of the finite wedges which cannot happen for infinite wedges.

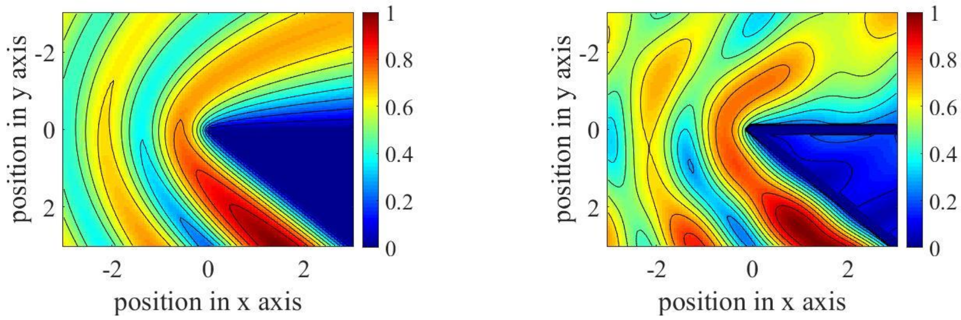

(analytical solution for infinite wedge, $k = 2$, $\theta_0 = \pi$, PEC surface, wedge angle is $\frac{\pi}{4}$) [31]
(a)

(proposed approach, $k = 2$, $\theta_0 = \pi, a_{1,2} = 2$, PEC surface, $\theta_0 = \pi$, wedge angle is $\frac{\pi}{4}$)
(b)

Figure 4. *Normalized near electric field distribution for the Wedge: different cases (a) infinite PEC-PEC wedge (b) finite PEC-PEC wedge*

In Figure 5, two cases (PEC-PMC and PMC-PMC) are provided. Besides, in Figure 5(c), a comparison with a computational electromagnetic approach called the method of auxiliary sources (MAS) is provided. The deviation is less than 2%. Notice that, the boundary condition has a huge effect on total radiation characteristics. In Figure 6, the comparison between the proposed approach and a single strip with different impedance boundary conditions on both sides is provided. In the limit cases, the impedance boundary condition can be assumed as PEC and PMC surfaces [32]. The near electric field distributions have deviation since the proposed geometry has two strips. The deviation from the comparison is expected because there exists a distance between the strips $l_{1,2} = 0.01$. In both figures, the upper strip (side) is PMC and the lower strip (side) is PEC. As it is seen, the boundary conditions, respectively, Neumann and Dirichlet boundary conditions for the upper and lower surface are satisfied. In Figure 7, comparisons are done regarding both methodology and boundary conditions. The methodologic comparison is done with the Method of Moment (MoM) and less than 4 % error is observed. Besides, parallelly located double-strip with fractional boundary condition [13] is compared with the proposed geometry with Dirichlet boundary condition. The deviation is found less than 2%. Besides, the oblique incidence case is compared in Figure 8 by MoM and fractional approach.

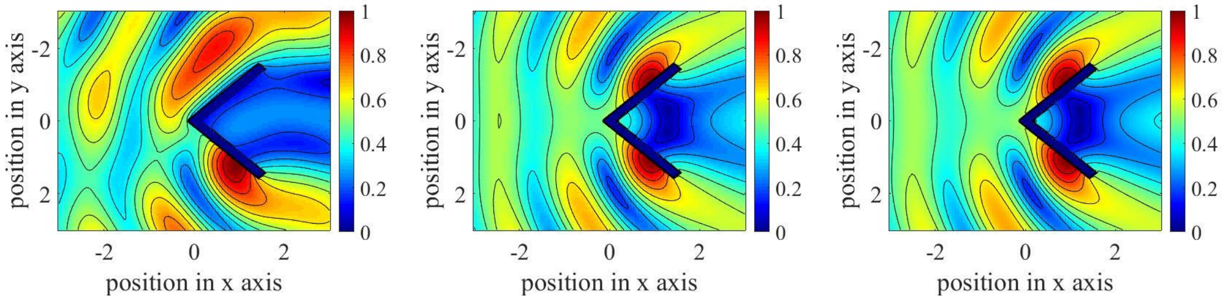

($k = 2, a_{1,2} = 1,\ \theta_0 = \pi,$ $\theta_{1,2} = \pm\frac{\pi}{4}, \phi_{1,2} = \pm\frac{\pi}{4}, l_{1,2} =$ 1.001, PEC-PMC)
(a)

($k = 2, a_{1,2} = 1,\ \theta_0 = \pi,$ $\theta_{1,2} = \pm\frac{\pi}{4}, \phi_{1,2} = \pm\frac{\pi}{4}, l_{1,2} =$ 1.001, PMC-PMC)
(b)

(MAS $k = 2, a_{1,2} = 1,\ \theta_0 = \pi,$ $\theta_{1,2} = \pm\frac{\pi}{4}, \phi_{1,2} = \pm\frac{\pi}{4}, l_{1,2} =$ 1.001, PMC-PMC)
(c)

Figure 5. *Normalized near electric field distribution for Finite Wedge: different cases (a) PEC-PMC (b) PMC-PMC (c) comparison of PMC-PMC with MAS*

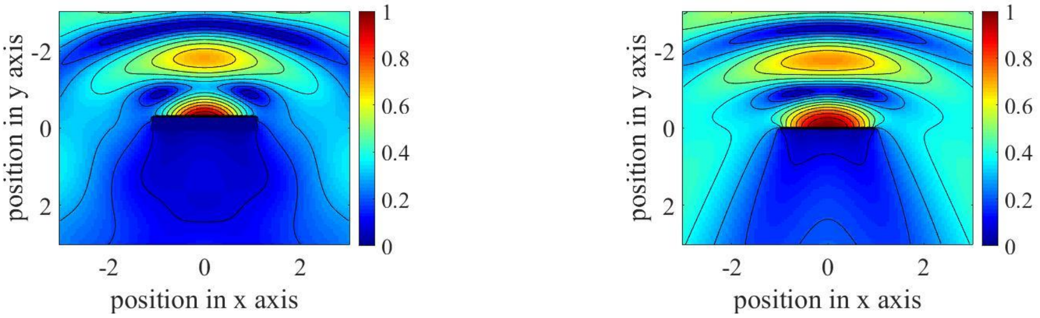

(The proposed approach, $l_{1,2} = 0.01$, $k = 2$, $a_{1,2} = 1,\ \theta_0 = \frac{\pi}{2}$, PMC, PEC)
(a)

(double-sided strip, $k = 2, a_{1,2} = 1,\ \theta_0 = \frac{\pi}{2}$, PMC, PEC) [32]
(b)

Figure 6. *Normalized near electric field distribution for a strip: different cases (a) The proposed approach (b) Impedance BC*

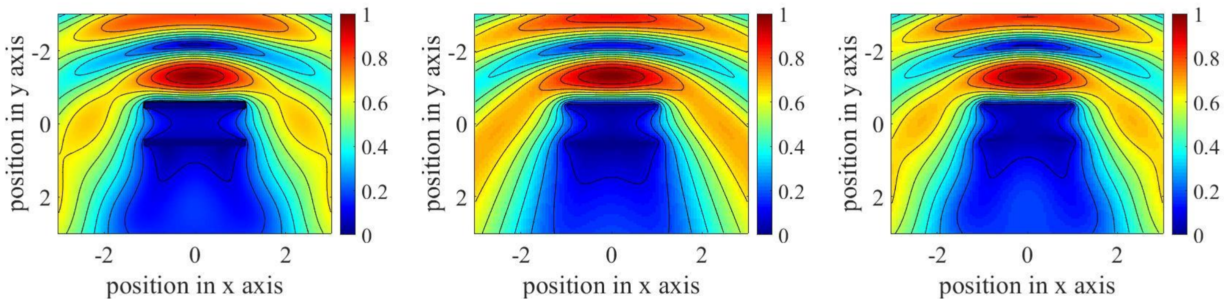

(The prosed approach, double strip, l=0.5 $k = 2, a_{1,2} = 1,$ $\theta_0 = \frac{\pi}{2}$, PEC-PEC)
(a)

(MoM approach, double strip, l=0.5 $k = 2, a_{1,2} = 1,\ \theta_0 =$ $\frac{\pi}{2}$, PEC-PEC
(b)

(Fractional approach, double strip, l=0.5 $k = 2, a_{1,2} = 1,$ $\theta_0 = \frac{\pi}{2}$, PEC-PEC)[13]
(c)

Figure 7. *Normalized near electric field distribution for double-strip: different cases (a) The proposed approach (b) MoM (c) Impedance BC*

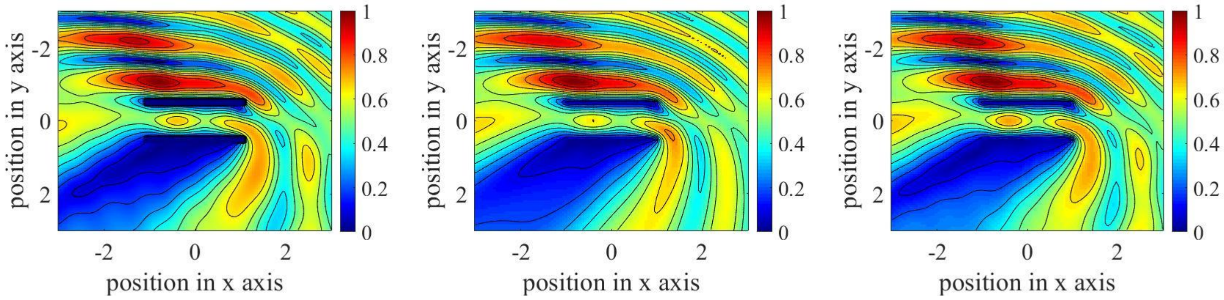

(Proposed approach, double strip, $l_{1,2} = 0.5$, $k = 4$, $a_{1,2} = 1$, $\theta_0 = \frac{\pi}{4}$, PEC, PEC)
(a)

(MoM approach, double strip, l=0.5 $k = 4$, $a_{1,2} = 1$, $\theta_0 = \frac{\pi}{4}$, PEC, PEC)
(b)

(Fractional approach, double strip, $l_{1,2} = 0.5$, $k = 4$, $a_{1,2} = 1$, $\theta_0 = \frac{\pi}{4}$, PEC, PEC) [13]
(c)

Figure 8. *Normalized near electric field distribution for double-strip: different cases (a) The proposed approach (b) MoM (c) Impedance*

4. CONCLUSION

The study investigates the E-polarized plane wave electromagnetic scattering by perfect electric and/or magnetic conducting double strips where the position, tilt angle, width, and boundary conditions (Dirichlet or Neumann) of the strips are the parameters and analyzed. The importance of the study can be summarized by the following two items. First, this study obtains approximate field distribution and physical characteristics of the finite wedge problems where two different surfaces may have different boundary conditions and widths. Secondly, the problem has been investigated for the first time with an orthogonal polynomials approach, and detailed comparisons and the advantages of the solution methodology are highlighted. The proposed method is semi-analytical-numerical and requires $ka + 5$ numbers of unknown for each strip to compute SLAE. This yields the advantages of a small dimensional matrix and inversion procedure since the edge condition is imposed by using the weighting function and Gegenbauer polynomials for the expression of the induced electric or magnetic currents on each strip. The outcomes are compared in the sense of both methodology and boundary conditions. As the methodology, analytical results, MoM, and MAS are employed to compare and results are coinciding. Besides, as the boundary conditions, the proposed approach is compared with the fractional and impedance boundary conditions. Again, high accuracy is obtained.

CONFLICTS OF INTEREST

No conflict of interest was declared by the authors.

REFERENCES

[1] Nethercote, M. A., Assier, R. C., and Abrahams, I. D., “Analytical methods for perfect wedge diffraction: a review”, Wave Motion, 93: 102479, (2020).

[2] Vinogradov, S. S., Smith, P. D., and Vinogradova, E. D., “Canonical problems in scattering and potential theory part II: Acoustic and electromagnetic diffraction by canonical structures”, Chapman and Hall/CRC, (2002).

[3] Bowman, J. J., Senior, T. B. A., and Uslenghi, P. L. E., “Electromagnetic and acoustic scattering by simple shapes (Revised edition)”, Hemisphere Publishing Corporation, New York, (1987).

[4] Alkumru, A., “Plane wave diffraction by three parallel thick impedance half-planes”, Journal of Electromagnetic Waves and Applications, 12(6): 801–819, (1998).

[5] Tabatadze, V., Karaçuha, K., Veliyev, E. I., and Karaçuha, E., "The Diffraction by Two Half-Planes and Wedge with the Fractional Boundary Condition", Progress in Electromagnetics Research M, 91: 1–10, (2020).

[6] Umul, Y. Z., "Scattering of electromagnetic waves by a perfect electromagnetic conductor half-screen", Optik, 181: 383–388, (2019).

[7] Daniele, V., Lombardi, G., and Zich, R. S., "The double PEC wedge problem: Diffraction and total far field", IEEE Transactions on Antennas and Propagation, 66(12): 6482–6499, (2018).

[8] Aydin, E. A., and İkiz, T., "Formulation of the Diffraction Problem of Almost Grazing Incident Plane Wave by an Anisotropic Impedance Wedge", Majlesi Journal of Telecommunication Devices, 3(3): 115-122, (2014).

[9] Basdemir, H. D., "Wave scattering by a perfect electromagnetic conductor wedge residing between isorefractive media", Progress in Electromagnetics Research M, 94: 31–39, (2020).

[10] Dikmen, F., Karacuha, E., and Tuchkin, Y. A., "Scalar wave diffraction by a perfectly soft infinitely thin circular ring", Turkish Journal of Electrical Engineering and Computer Sciences, 9(2): 199–220, (2001).

[11] Of, J., April, E., and Chunfei, Y., "New approach to electromagnetic scattering from a conductive disc-ring structure", Chinese Journal of Electronics, 12(2): 168-176, (1995).

[12] Lee, H. S., and Eom, H. J., "Electromagnetic scattering from a thick circular aperture", Microwave and Optical Technology Letters, 36(3): 228–231, (2003).

[13] Tabatadze, V., Karaçuha, K., and Veliyev, E. I., "The solution of the plane wave diffraction problem by two strips with different fractional boundary conditions", Journal of Electromagnetic Waves and Applications, 34(7): 881–893, (2020).

[14] Karaçuha, K., Tabatadze, V., and Veliyev, E. I., "Electromagnetic plane wave diffraction by a cylindrical arc with edges: H-polarized case", International Journal of Applied Electromagnetics and Mechanics, 68: 13–27, (2022).

[15] Sefer, A., and Yapar, A., "A spectral domain integral equation technique for rough surface scattering problems", Waves in Random and Complex Media, 31(6): 1523–1539, (2021).

[16] Karaçuha, K., Tabatadze, V., and Veliev, E. I., "Plane wave diffraction by strip with an integral boundary condition", Turkish Journal of Electrical Engineering and Computer Sciences, 28(3): 1776–1790, (2020).

[17] Zinenko, T. L., and Nosich, A. I., "Plane wave scattering and absorption by flat gratings of impedance strips", IEEE Transactions on Antennas and Propagation, 54(7): 2088–2095, (2006).

[18] Polat, B., and Daşbaşı, R., "Free space doppler analysis and RCS of a moving PEC plate under physical optics approximation", IEEE 2021 8th International Conference on Electrical and Electronics Engineering (ICEEE), 27-31, (2021).

[19] Koç, U. C., Başaran, E., Ülkü, H. A., and Alkumru, A., "Hareketli Bir Küreye İlişkin Enerji Dağılımı ve Saçılma Katsayısı", URSI-Türkiye 2021 X. National General Assembly, (2021).

[20] Gürbüz, T. U., Aslanyürek, B., "A Semi-Analytical Method for Electromagnetic Scattering by Infinitely Long Arbitrary Shaped Multilayer Cylinders at Oblique Incidence", IEEE Transactions on Antennas and Propagation, (2023).

[21] Nagasaka, T., and Kobayashi, K., "Wiener-Hopf Analysis of the Diffraction by a Strip with Fractional Boundary Conditions", 2019 Photonics & Electromagnetics Research Symposium-Fall, 66–72, (2019).

[22] Butler, C., "General solutions of the narrow strip (and slot) integral equations", IEEE Transactions on Antennas and Propagation, 33(10): 1085–1090, (1985).

[23] Ziolkowski, R., and Grant, J., "Scattering from cavity-backed apertures: The generalized dual series solution of the concentrically loaded E-pol slit cylinder problem", IEEE Transactions on Antennas and Propagation, 35(5): 504–528, (1987).

[24] Karaçuha, K., Tabatadze, V., Alperen, Ö.F., Karaçuha, E., and Veliev, E., "Electromagnetic Diffraction by a Slotted Cylinder with the Fractional Boundary Condition", Progress in Electromagnetics Research C, 128: 61-71, (2023).

[25] Meixner, J., "The behavior of electromagnetic fields at edges", IEEE Transactions on Antennas and Propagation, 20(4): 442–446, (1972).

[26] Bateman, H., Higher transcendental functions, McGraw-Hill Book Company, New York, (1953).

[27] Prudnikov, A. P., Brychkov, I. A., and Marichev, O. I., Integrals and series: special functions, 2, CRC Press, (1986).

[28] Tabatadze, V., Karaçuha, K., Alperen, Ö. F., and Veliev, E., "H-polarized plane wave diffraction by a slotted cylinder with different surface impedances: Solution by the analytical—Numerical approach", IET Microwaves, Antennas & Propagation, 16(14): 869-79, (2022).

[29] Balanis, C. A., Antenna theory: analysis and design, John Wiley & Sons., (2016).

[30] Ishimaru, A., Electromagnetic wave propagation, radiation, and scattering: from fundamentals to applications, John Wiley & Sons., (2017).

[31] Balanis, C. A., Advanced Engineering Electromagnetics, John Wiley & Sons., (1999).

[32] Tabatadze, V., Karacuha, K., Karacuha, E., and Veliev, E., "Electromagnetic Scattering by the Strip with Different Impedances on Both Sides", 2022 IEEE 2nd Ukrainian Microwave Week (UkrMW), 482-485, (2022).